Hindawi
Cellular Microbiology
Volume 2023, Article ID 6868417, 14 pages
https://doi.org/10.1155/2023/6868417

Research Article

Fecal Microbiome Does Not Represent Whole Gut Microbiome

Ji-Seon Ahn,[1,2] **Enkhchimeg Lkhagva**,[1] **Sunjun Jung**,[3] **Hyeon-Jin Kim**,[4] **Hea-Jong Chung**,[2] **and Seong-Tshool Hong**[1]

[1]*Department of Biomedical Sciences and Institute for Medical Science, Jeonbuk National University Medical School, Jeonju, Chonbuk 54907, Republic of Korea*
[2]*Gwangju Center, Korea Basic Science Institute, Gwangju 61751, Republic of Korea*
[3]*College of Veterinary Medicine, Jeonbuk National University, Iksan, Chonbuk 54596, Republic of Korea*
[4]*JINIS BDRD Institute, JINIS Biopharmaceuticals Co., 224 Wanjusandan-6-Ro, Bongdong, Wanju, Chonbuk 55315, Republic of Korea*

Correspondence should be addressed to Hea-Jong Chung; hjchung84@kbsi.re.kr and Seong-Tshool Hong; seonghong@jbnu.ac.kr

Received 12 October 2022; Revised 20 December 2022; Accepted 2 January 2023; Published 17 January 2023

Academic Editor: Jayaprakash Narayana Kolla

The current gut microbiome research relies on the fecal microbiome under the assumption that the fecal microbiome represents the microbiome of the entire gastrointestinal (GI) tract. However, there have been growing concerns about using feces as a proxy to study the gut microbiome. Here, we comprehensively analyzed the composition of microbiome and metabolites in the feces and at 14 different locations of GI tracts of genetically homogenous sibling pigs to evaluate the validity of using feces as a proxy to the whole gut microbiome. The composition of intestinal microbes constituting the gut microbiome at each intestinal content and feces and their metabolic compositions were thoroughly investigated through metagenome sequencing and an ultraperformance LC-MS/MS, respectively. The fluctuation in the composition of the microbiome in the stomach and the small intestine became stabilized from the large intestine to feces and was able to be categorized into 3 groups. The taxonomic α-diversities measured by ACE (abundance-based coverage estimator) richness and Shannon diversity indicated that the microbiome in the large intestine was much more diverse than those of the small intestine and feces. The highly independent intestinal microbes in the stomach and the small intestine became flourished in the large intestine and converged into a community with tightly connected networks. β-Diversity analyses by NMDS plots, PCA, and unsupervised hierarchical clustering all showed that the diversities of microbiome compositions were lowest in feces while highest in the large intestine. In accordance with fluctuation of the composition of gut microbiome along with the GI tract, the metabolic composition also completely differed in a location-specific manner along with the GI tract. Comparative analysis of the fecal microbiome and metabolites with those of the whole GI tract indicated that fecal microbiome is insufficient to represent the whole gut microbiome.

1. Introduction

The mammalian intestines contain a massive and complex microbial community called gut microbiome which consists of 100 trillion individual microbes [1]. Gut microbiome has been known to play a significant determinant role in phenotypes and diseases of its host [2]. Thus, the elucidation of the determinant role of the gut microbiome on phenotypes and diseases has gained growing attention for opportunities for pharmabiotic applications [3, 4]. It is obvious that gut microbiome affects the phenotypes and diseases of its host potentially as much as their own genomes [5–9]. Despite the clear evidence of its determinant roles, the detailed mechanisms on the role of gut microbiome have not investigated as expected.

The first step to elucidate the action mechanism of gut microbiome on its host would depend on the identification of individual microbes at a species level. Identification of individual intestinal microbes affecting the phenotypes and diseases depends on statistical analyses between two main variables. One variable is the composition of gut microbiome, and the other is phenotypes or diseases of interest. Because the phenotypes or diseases are typically well-defined, the success of statistical analyses on these studies

would depend on precise elucidation of the composition of gut microbiome. Therefore, it cannot be overestimated to determine gut microbiome precisely without sampling variation [10–12].

It has been generally assumed that fecal sample is a proxy of the whole gut microbiome. However, recent findings made this general baseline assumption to be questionable [13–15]. The assumption based on not only that stool consistency is universally maintained but also that the chemical composition and physical environment within the GI tract are essentially similar. However, individual stool consistency varies over time. And, obviously, the chemical composition and physical environment in the GI tract differ in a location-specific manner. In fact, it has shown that the composition of gut microbiome of a same individual was significantly different at varying time points and sampling methods. The daily variance of the composition of gut microbiome relied on the stool consistency [13–15], suggesting that single fecal sampling to represent an individual's microbiota could differ vastly depending on a given time point. Furthermore, recent studies showed that the gut microbiome analyzed by using the signature of blood plasma was completely different from the gut microbiome directly through fecal samples, indicating a possibility that the microbiome in feces would not represent the whole gut microbiome of the individual [16, 17].

The reason behind the heavy variance of gut microbiome composition depending on the stool samples at different moments or sampling areas has not been understood. Here, we showed that the heavy variance of gut microbiome depending on the stool sampling is due to phenomenon of the compositional difference of gut microbiome in a location-specific manner along the GI tract. This work signifies not only the consistent sampling method considering stool consistency to minimize the inevitable error of current gut microbiome analyses but also development of a new technology elucidating the accurate composition of whole gut microbiome.

2. Methods

2.1. Animals and Sample Collection. In accordance with the ethical guidelines of the Ethics Committee of Jeonbuk National University Laboratory Animal Center (Permit Number: CBU 2012-0040), all experiments with animals were performed with the "Guide for the Care and Use of Laboratory Animals," published by the National Research Council (ARRIVE Guidelines). The feces and intestinal contents were obtained from three, 49-day-old, healthy male Landrace pigs of the same littermates of similar weight which fed the same diet and housed in an environmentally controlled room. Pigs were ad libitum fed with fodder based on maize and soybean and mixed grain with 3,600 kcal energy and crude protein less than 21.0%. During the experiment, all pigs were not exposed to any antibiotics, high zinc/copper, probiotics, or any other agent which are being known to modulate the microbiome.

Each pig was transferred to a single pen just before euthanasia, and the feces was collected while fasted in the pen for two hours. The pigs were electrically stunned with 250 V using an automatic high-voltage stunning device. Immediately after electrical stunning, the necks of the pigs were dislocated to isolate the whole GI tract. The GI tract was immediately removed after euthanasia from the abdominal cavity. Right after isolation of the whole GI tract, the luminal contents in each location were collected. The GI tract was divided into 14 parts based on the anatomical structure: 1 part of the stomach, 6 parts of the small intestine, and 7 parts of the large intestine [18, 19]. The anatomical differences between each location were shown in Supp. Figure 1. From each animal, the luminal contents of the 14 sections were collected individually after isolating ~10 cm of each section using clamps on each side. Afterward, an incision was made in the middle of each section with a scalpel aseptically. Finally, a sterile micro spatula with a large opening was used to collect luminal content through the incision. The collected luminal contents were transferred to falcon tubes. Each sample was weighed and immediately frozen in liquid nitrogen and stored at −80°C until used. The mean lengths of the stomach, the small intestine (6 parts), and the large intestine (7 parts) were measured.

2.2. Determination of Water Content and pH of the Gastrointestinal Tract. The water content in the GI tract was determined based on the wet and dry weight of each sample. For this purpose, the dry mass was recorded after lyophilization and compared to the wet weight of each sample. The pH values of the contents of each gastrointestinal tract segment were determined immediately after sample collection (Orion Star™ A210 pH meter, Fisher Scientific, USA). The pH was measured at least three times with thorough mixing of the contents of the GI tract.

2.3. LC-MS/MS Analysis. Unbiased metabolomics analysis was carried out with an ultraperformance liquid chromatography (UPLC) system (Waters, MA, USA) as described previously [20]. Briefly, the chromatographic separation was done at a column temperature of 40°C and a flow rate of 0.5 mL/min with the ACQUITY UPLC HSS T3 column (100 × 2.1 mm, 1.8 μm, Waters, MA, USA), in which the mobile phase contained solvent A (water containing 0.1% formic acid) and solvent B (acetonitrile containing 0.1% formic acid). The gradient elution conditions for the metabolites were 97% phase A for 0 ~ 5 min, 3 ~ 100% liner gradient phase B for 5 ~ 16 min, 100% phase B for 16~17 min, 100~3% reverse liner gradient phase B for 17~19 min, and 97% phase A for 19~25 min. The loading volume was 5 μL for each sample. The eluted metabolites were detected by a high-resolution tandem mass spectrometer SYNAPT G2 Si HDMS QTOF (Waters, USA). The capillary voltage and the cone voltage were 2 kV and 40 V, respectively, for the positive ion mode. For the negative ion mode, the capillary voltage and the cone voltage were 1 kV and 40 V, respectively. The mass spectrometry data was collected with centroid MSE mode. The scanning time was 0.2 seconds, and the primary scans were from 50 to 1200 Da. The parent ions were fragmented at 20~40 eV. The

information of all fragments was collected, and the time was 0.2 second. For real-time quality correction, the LE signal was gained every 3 seconds in the data acquisition process. Leucine enkephalin at a flow rate of 10 μL/min was used as a lock mass by a lock spray interface to monitor the positive ion modes ($[M + H] + = 556.2771$) and the negative ion modes ($[M - H] - = 554.2615$).

2.4. Data Processing and Metabolite Identification. The obtained mass spectrometry data were processed and extracted to identify peaks through chromatogram alignment, peak picking, peak area extraction, and normalization using commercial software Progenesis QI (version 2.2; Waters, MA, USA) implementation. Potential markers of interest were extracted from S-plot (EZinfo software 2.0), which was constructed following the analysis with partial least squares discriminant analysis (PLS-DA). Markers were chosen based on their contribution to the variation and correlation within the dataset. To identify biomarkers, the ion spectrum of potential biomarkers was matched with the structure message of metabolites acquired from available biochemical databases such as MassBank (http://www.massbank.jp/), HMDB (http://www.hmdb.ca/), LIPID MAPS (http://www.lipidmaps.org/), and METLIN (http://metlin.scripps.edu/). The reconstruction, interaction, and pathway analysis of potential biomarkers were carried out with MetPA online (http://metpa.metabolomics.ca) to identify the metabolic pathways. MetPA used the high-quality KEGG metabolic pathways as the backend knowledge base.

2.5. 16S rRNA Gene Sequencing. Total genomic DNA was extracted from each sample using the standard extraction protocol as described previously [21, 22]. Briefly, samples suspended in lysis buffer (200 mM NaCl, 200 mM Tris-HCl (pH 8.0), and 20 mM EDTA) were lysed by bead beating. Genomic DNA was recovered from the aqueous phase by extraction with phenol, chloroform, and isoamyl alcohol. DNA was precipitated with the addition of 3 M sodium acetate followed by isopropanol. After rinsing with 70% ethanol, the dried DNA pellet was dissolved in TE buffer (10 mM Tris-HCl pH 8.0 and 1 mM EDTA). The concentration and purity of the DNA were measured using a BioSpec-nano spectrophotometer (Shimadzu Biotech, Kyoto, Japan) followed by analysis on 1% (w/v) agarose gel electrophoresis. Each sequencing sample was prepared according to the Illumina 16S Metagenomic Sequencing Library protocols. The 16S rRNA genes were amplified using 16S V3-V4 primers: 16S amplicon PCR forward primer (5′TCGTCGGCAGCGTCAGATGTGTATA AGAG ACAGCCTACGGG-NGGCWGCAG3′) and 16S amplicon PCR reverse primer (5′GTCTCGTGGGCTCGGAGATGT GTATAAGAGACAGGACTACHVGGGTATCTAAT CC3′). Input genomic DNA was also amplified with 16S V3-V4 primers followed by subsequent amplification step to add multiplexing indices and Illumina sequencing adapters. The final products were normalized using the PicoGreen. The size of libraries was verified using the TapeStation DNA screentape D1000 (Agilent, CA, USA). Then, sequencing (2×300) was done with the MiSeq™ platform (Illumina, CA, USA). The amplicon error was modeled using DADA2. Errors in marginal sequences were corrected. Chimeric sequences and singleton were also removed, followed by dereplication of those sequences [22]. The raw data were deposited in the public repository at NCBI SRA with accession number PRJNA707378 (https://submit.ncbi.nlm.nih.gov/subs/sra/).

2.6. Data and Statistical Analyses. All data and statistical analyses were determined as described previously [21, 22]. In brief, the Q2-Feature classifier is a Naive Bayes classifier based on the SILVA (region V3-V4) database (https://www.arb-silva.de/). We used the program to classify our datasets after setting denoise-single function as default parameter. The q2-diversity under the option of "sampling-depth" was used for the diversity calculation and statistical tests. We employed a sequencing quality score threshold of at least 20, and rarefaction depth was 11,510. After confirming the quality of sequencing results, the sequencing results in "table.qzv" files were filtered by using the threshold values in QIIME 2. For visualization of alpha and beta diversities, the metagenomic data OTU and taxonomic classification tables were imported into phyloseq (1.28.0) package (R version 3.6.1). Statistical analysis was done using the Kruskal-Wallis rank sum test for alpha diversity. For beta diversity, we used permutational multivariate analysis of variance (PERMANOVA) in the vegan package of the R version [23]. Analysis of dissimilarity (ADONIS) was used with 999 permutations in the vegan package of R version to quantify the effect size of variables explaining the Bray-Curtis distance. All P value was corrected by Benjamini and Hochberg's adjustment, and significance was declared at $P < 0.05$.

2.7. Reconstitution of the Whole Gut Microbiome. Since the intestinal matters of individual pigs were too big for quantification of the whole gut microbiome, we reconstituted the whole gut microbiome by multiplying the density value by the OTUs at each site after quantification of total bacterial numbers using a real-time quantitative PCR method. Total bacterial genomic DNA from each of the intestinal matters at the 14 sites was extracted with phenol-chloroform and isoamyl alcohol as described previously, using equivalent weights of each sample for the real-time PCR and metagenome sequencing. The isolated bacterial genomic DNAs were quantitated by real-time PCR by using the PicoReal real-time PCR instrument (Thermo Fisher Scientific, NH, USA). iQ SYBR Green supermix (Bio-Rad Laboratories, CA, USA) was used to quantitate the synthesized DNAs during the real-time PCR. Each 10 μL of the reaction mixture contained 5 μL of iQ SYBR Green supermix, 100 nM of the universal primers for 16S rRNA (forward primer: 341F CCT ACG GGA GGC AGC AG and reverse primer: 534R ATT ACC GCG GCT GCT GGC A), and 50 ng of the template DNA. The real-time PCR cycle condition was 1 cycle of 95°C for 5 min; 40 cycles of 95°C for 15 s, 58°C for 30 s, and 72°C for 30 s; and final 1 cycle of 60°C for 30 s. The melting curves were obtained by slow heating at temperatures from

60°C to 95°C at a rate of 0.2°C per second with continuous fluorescence collection.

After quantitation of the total bacterial number at each site, the number was divided by the total number of OTUs at the site to get a multiplication value. Each of the multiplication value was divided by the weight of samples to represent the multiplication value per g. After getting the multiplication value per g, the value at each site was multiplied by individual OTU numbers to get the actual numbers of the individual OTUs at each site. All the OTUs in each 14 intestinal matters were combined together to reconstruct the whole gut microbiome of each pig as a value of per gram.

2.8. The α-Diversity Analysis for Relative Abundance Evaluation of Material and Microbiome. The α-diversity analysis for relative abundance was determined as described previously [21, 22]. The α-diversity metrics for the Shannon index and abundance-based coverage estimator (ACE) were calculated without filtering in phyloseq package [24]. Core metric analysis was used to detect any differences in the richness and alpha diversity between groups. Cumulative sum scaling (CSS) normalization implemented in the R package metagenome Seq before converted into relative abundance. Any taxa, at family level, with a total of <0.5% were collapsed into "other."

2.9. The β-Analysis for Relative Abundance of Material and Microbiome. In the phyloseq package using the Bray-Curtis dissimilarity, the β-diversity metrics were computed and visualized using log-transformed, normalized OTU data described previously [21, 22]. The unweighted UniFrac metric was used for β-diversity. PCoA was calculated and visualized by the vegan package [23]. A nonmetric multidimensional scaling (NMDS) was plotted in the phyloseq (1.28.0) package (R version 3.6.1). The significances of β-diversity metrics were tested by analysis of dissimilarity (ADONIS) with 999 permutations by the vegan package of R version [23].

2.10. Heatmap and Phylogenetic Tree. Sample clustering was performed using seaborn 0.9.0. (http://seaborn.pydata.org) as described previously [21, 22]. Briefly, the hierarchical cluster analysis was carried out with Euclidean distance correlation as the distance measurement with average linkage. Clusters were visualized via cluster map of seaborn. We calculated the Bray-Curtis dissimilarity matrix using "vegan" and reduced the range by taking log2 of the calculated values. The OTUs were correlated using the stats package, and heatmaps were visualized with the ggplot2 package. The average linkage, hierarchical clustering, and Bray-Curtis distance matrix were used for cluster analysis and heatmap construction, respectively.

Phylogenetic trees for each sampling site were constructed from raw sequences without filtering so that they can show direct visualization of sample richness with relation to taxonomy classification [21, 22]. Briefly, 16S rRNA sequences from each sampling site were aligned using a ClustalW program with default parameters. The resulting alignments were used to construct the maximum-likelihood phylogenetic trees in MEGAX with 500 bootstrap replicates. The phylogenetic trees were visualized with iTOL.

2.11. Cooccurrence Network Construction. Coabundance network was constructed by a permutation-renormalization-bootstrap network construction strategy as described previously [19, 20] to observe the microbial cooccurrence relationships in a GI tract as well as feces. Nonnormalized abundance data was uploaded to the CoNet program, a Java Cytoscape plug-in. All networks were independently constructed by splitting the OTU abundance matrix of the stomach, the small intestine, the large intestine, and feces groups. The microbial networks and links were obtained from OTU occurrence data. Multiple ensemble correlation methods in the CoNet program were used to identify significant copresences across the samples while OTUs that occurred in less than two samples were discarded ("row_minocc" = 2). Five similarity measures, including the Spearman and Pearson correlation coefficients, the mutual information score, and the Bray-Curtis and Kullback–Leibler dissimilarities, were calculated by CoNet program to create an ensemble network without P value merge. The P value was corrected by the Benjamini–Hochberg correction method with an adjusted P value of less than 0.05. If at least two of the five metrics suggested significant coabundance between the two OTUs, the relationship was kept as an edge in the final network. The final cooccurrence network model was displayed by the igraph package in the R version by using an implementation of the Louvain algorithm to identify communities within each network to maximize the modularity score of each OTU within a given network.

2.12. Quantification and Statistical Analysis. All statistical analyses are reported as mean ± SEM. The differences in the relative abundance of bacterial populations among GI parts and feces were analyzed using the Kruskal-Wallis rank sum test in the R software. Significance was considered at $P < 0.05$ with Benjamini and Hochberg's adjustment. All graphs were prepared with the R software.

3. Results

3.1. The Composition of Gut Microbiome Differed in a Location-Specific Manner. Heavy variance of gut microbiome composition depending on stool consistency prompted us to investigate the profile of gut microbiome at each location in the GI tract. Since small animals make it very difficult for isolation of intestinal matter in a location-specific manner, the study was conducted using pigs, which are omnivorous and have most similar digestive mechanisms to human among the animal kingdoms.

A total of 137,695 ± 2,607 OTUs were generated by sequencing the V3-V4 sites of the 16S rDNA of the gut microbiome at the 14 sites and feces of each pig. The OTUs were grouped into 9,431 ± 559 OTUs by matching with the SILVA (region V3-V4) database (https://www.arb-silva.de/) after removing low-quality sequences or chimeras (Supp. Table 1). The gross microbiome analysis at the phylum level indicated that the composition of the microbiome

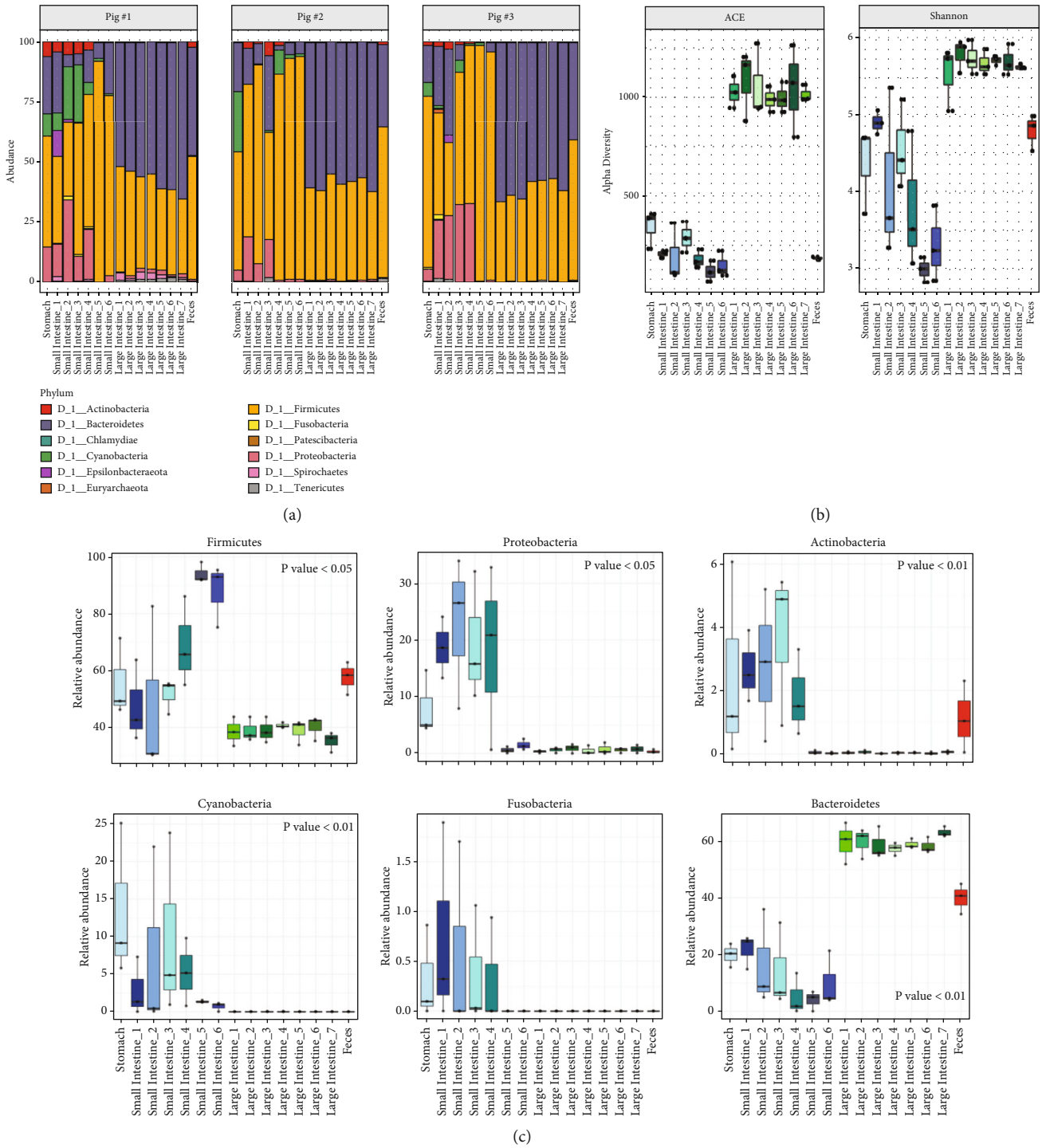

FIGURE 1: The microbial diversity at each location of the GI tract by α-diversity analysis. (a) The relative abundance of microbial phyla at each location of GI tract and feces. (b) Species richness and diversity were measured by the ACE and Shannon ($P < 0.05$). (c) The relative abundances of the predominant intestinal microbes at phylum level which are Firmicutes, Proteobacteria, Actinobacteria, Cyanobacteria, Fusobacteria, and Bacteroidetes. The sampling locations within the GI tract were determined based on the anatomical feature: the stomach, the duodenum (small intestine_1), the jejunum (small intestine_2 ~ small intestine_5), the ileum (small intestine_6), the cecum (large intestine_1), the colon (large intestine_2 ~ large intestine_6), and the rectum (large intestine_7). The anatomical differences between each location are shown in Figure S1.

constantly changed along the GI tract although Firmicutes and Bacteroidetes were the two main phyla in each location (Figure 1(a) and see Supp. Table 2). *Unclassified_ Lactobacillus_sp* was most dominant in the stomach and the small intestine sites, while site-wise *Unclassified_ Staphylococcus sp.* in the stomach, Lactobacillus mucosae and

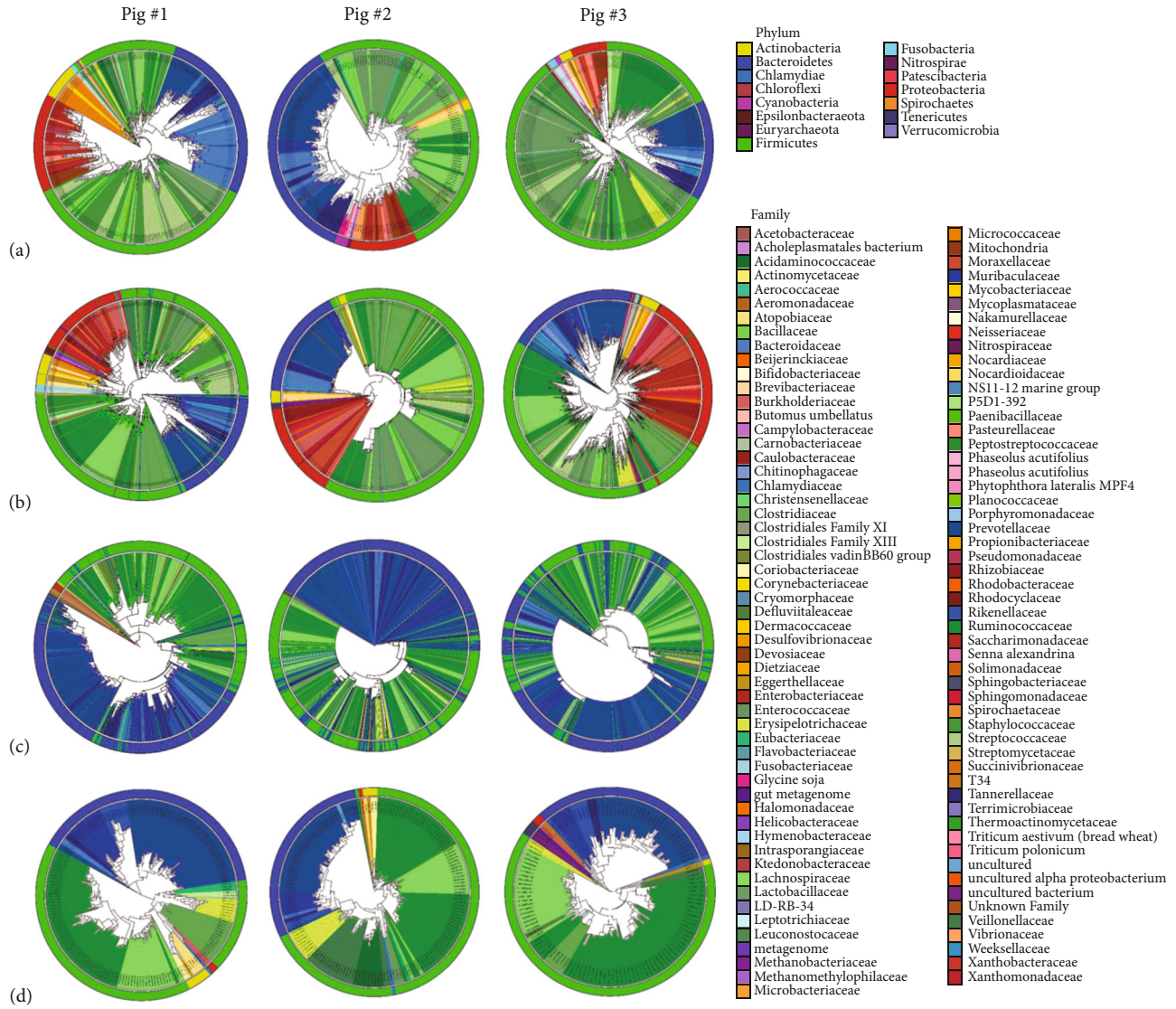

FIGURE 2: Maximum-likelihood phylogenetic tree comprising of the taxa at the stomach (a), the small intestine (b), and the large intestine (c) of the GI tract and feces (d) of pigs #1 ~3. Clades are labeled according to the species. Phylum is depicted in the first outer layer and brunch node. Inner circle color represents the family level.

Helicobacter rappini in the small intestine #1, *Unclassified_Chloroplast_sp* and *Unclassified_Mitochondria_sp* in the small intestine #2, *Escherichia-Shigella and Phaseolus acutifolius* in the small intestine #3, *Unclassified_Streptococcus_sp* in the small intestine #4, *Unclassified_Terrisporobacter_sp* in the small intestine #5 and the small intestine #6, and *Unclassified_Clostridium sensu stricto 1*; uncultured bacterium in lower sites of the small intestine #3~5 was dominant. *Unclassified_Prevotellaceae_sp* and *Porphyromonadaceae bacterium DJF_B175* were dominant through the large intestine, and *Unclassified_Lachnospiraceae_sp* and *uncultured Prevotella sp.* were evenly distributed in each site of the large intestine even with small abundance. *Unclassified_Faecalibacterium_sp* and *Unclassified_Prevotella 9_sp* were abundant in feces (Supp. Table 3).

The α-diversity measurements showed that the microbiome in the large intestine was much more diverse than those of the small intestine and feces (Figure 1(b)). The diversity indexes indicated that the gut microbiome was most diverse in the large intestine and least diverse in the stomach and the small intestine, with fecal microbiome showing medium diversity. The microbiome in the stomach and the small intestine which are rich in nutrients was very different from the gut microbiome of the large intestine and feces in terms of both composition and diversity (Figures 1(a) and 1(b) and Supp. Table 4). Visualization of the individual phylum's relative abundance further validated the observation that the whole gut microbiome can be grouped into 3 categories. Firmicutes, Proteobacteria, Actinobacteria, Cyanobacteria, and Fusobacteria were relatively more dominant in the stomach—the small intestine than the large intestine and feces. Bacteroidetes was more heavily dominated in the large intestine and feces than the stomach—the small intestine (Figure 1(c)).

Figure 2 shows the maximum phylogenetic tree which included all the species detected at each location. Although the gut microbiome differed in a location-specific manner, the maximum likelihood phylogeny analysis of Figure 2 was essentially in agreement with the gross analysis result at a phylum level of Figure 1. The gut microbiome between locations within a same individual was significantly different while the individual difference of the gut microbiome at the same locations of the GI tract was not as significant (Supp. Figure 2).

3.2. The Composition of Gut Microbiome in the GI Tract Fluctuated from the Stomach to the Small Intestine but Became Stabilized from the Large Intestine to Feces. After gross analysis of the microbiome in the GI tract and feces, we further analyzed the microbiome composition at lower taxonomic levels (Figure 3 and Supp. Table 5). The composition of the gut microbiome heavily fluctuated from the stomach to the small intestine so that the composition changed location to location (Figure 3(a)). However, the fluctuated microbiome became stabilized starting from the large intestine and remained fairly constant to feces. The composition of gut microbiome from the stomach to the midregion of the small intestine (the small intestine 4) has fluctuated significantly, and the gut microbiome was individually different (Figure 3(b)). It was very interesting to note that Clostridiaceae in the distal region of the small intestine (the small intestines 5 and 6) suddenly flourished in all of the 3 individual pigs, suggesting that the local environment of the region is optimal for the growth of Clostridiaceae. Unlike the microbiome from the stomach to the small intestine, the composition of gut microbiome was maintained consistently to the rest of the large intestine, indicating that the microbiome became stabilized from the large intestine. Prevotellaceae, Ruminococcaceae, and Tannerellaceae were the top 3 abundant families in the gut microbiome of the large intestine while Prevotellaceae, Ruminococcaceae, and Lachnospiraceae were the top 3 abundant families in the fecal microbiome (Figure 3 and Supp. Table 5). Although the fecal microbiome was quite similar to the gut microbiome of the large intestine, there was a clear difference in the gut microbiome of feces and the large intestine in all of the 3 individual pigs, confirming that the whole gut microbiome can be grouped into three categories (Supp. Figure 3).

3.3. The β-Analysis Visualized the 3 Categories of the Whole Gut Microbiome. Unsupervised hierarchical clustering of all locations at the genus level based on the Bray-Curtis distance matrix revealed that there were not any dominant genera across all of the locations (Figure 4(a)). Rather, each location has unique distribution of intestinal microbes, indicating a location-specific composition of gut microbiome. Nonetheless, the unsupervised hierarchical clustering analysis visualized the gut microbiome into three patterns: the stomach to the small intestine, the large intestine, and feces. Despite a pattern difference among the three categories of the gut microbiome, the fecal microbiome was more closely related to the gut microbiome in the large intestine than the stomach or the small intestine.

The mean distance to the centroid of the gut microbiome by β-diversity measurement was highest in the large intestine and lowest in feces, indicating the highest structural variation of the gut microbiome in the large intestine (Figure 4(b)). Visualization of the gut microbiome by principal coordinates analysis (PCoA) showed that the structures of the gut microbiome within the large intestine were essentially the same while the other parts differed from each other (Figure 4(c)). An NMDS biplot revealed that Firmicutes and Bacteroidetes are the two dominant phyla and are universally present in all of the 14 locations and feces. The biplot also showed that the gut microbiome can be grouped into three categories: the stomach to the small intestine, the large intestine, and feces (Figure 4(d) and Supp. Table 6 ~ 8).

3.4. The Chemical Profile in the GI Tract Differed in a Location-Specific Manner. The chemical compositions of GI contents were also investigated by analyzing the metabolites of the GI contents using an ultra-high-resolution LC-MS/MS. Unbiased metabolomics analysis was performed using an ultraperformance liquid chromatography (UPLC) system with the ACQUITY UPLC HSS T3 column. A total of 827 different chemical compounds were detected, and the chemical compositions at each GI location were different from each other while the feces showed the least chemical diversity (Supp. Figure 4 and Supp. Table 9). The average chemical diversities and distributions of the GI contents were statistically analyzed by α-diversity calculation (Supp. Table 9). The α-diversity indices showed that chemical compounds in each GI location were very different from each other (Supp. Figure 4). As expected, feces had the least chemical diversity with an uneven distribution of chemicals, indicating that feces consisted of much less diverse chemicals with the dominance of major compounds unlike the GI contents.

The variation in chemical composition along the GI tract was further analyzed by the β-diversity analysis method. In agreement with the α-diversity analysis result, the chemical composition of the feces was different in a location-specific manner (Figure 5). Unsupervised hierarchical clustering of all locations on chemical profiles based on the Bray-Curtis distance matrix revealed that each location has a unique chemical profile, indicating a location-specific composition of chemicals (Figure 5(a)). Unlike the profiles of the gut microbiome, the unsupervised hierarchical clustering analysis categorized the chemical profiles in the GI tract into two groups. The chemicals in the stomach, feces, and small intestine were categorized as a group, and the chemicals in the large intestine were categorized as the other group. Considering that the uptake of food in the stomach consists of mostly undigested macromolecules which cannot be detected by LC-MS/MS, it would not be surprising to find a similarity of the chemical profiles between the stomach and feces in the Bray-Curtis distance matrix (Figure 5(a)).

The mean distance to the centroid of the chemical composition at each site by β-diversity measurement showed that the large intestine contained the highest amount of

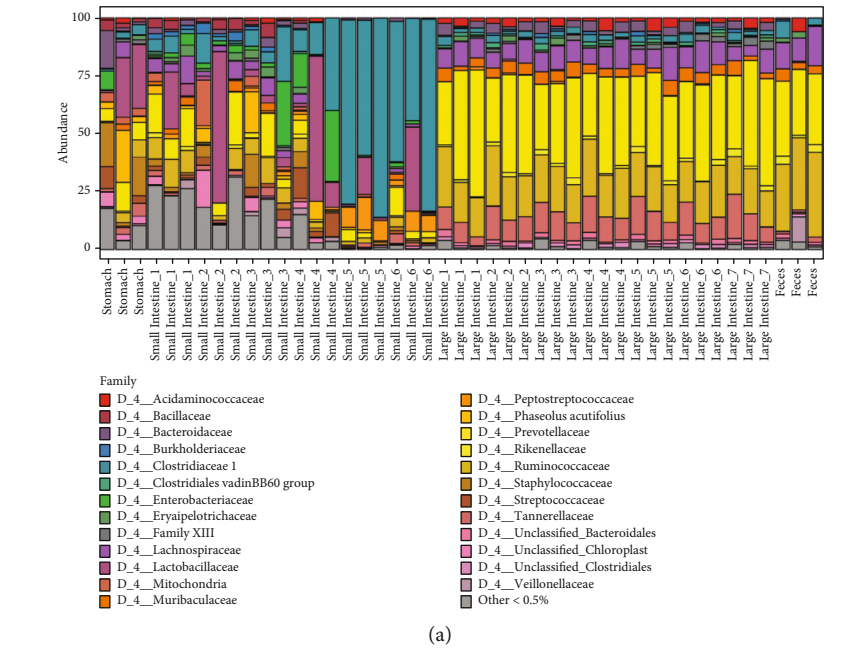

(a)

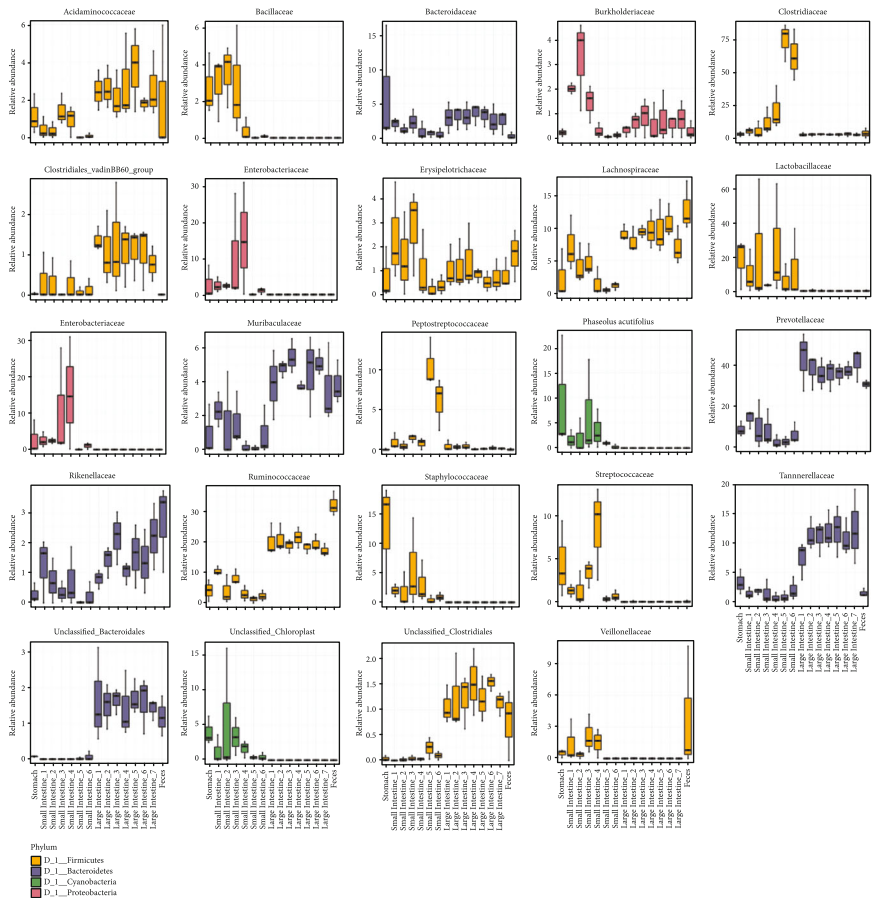

(b)

Figure 3: Relative abundances of sequences belonging to different families in the GI tracts. (a) The relative abundance of families at 14 locations of GI tract and feces. (b) The boxplots of the most abundant families for all through samples. Plot color represents the phylum level of families. The sampling locations within the GI tract were determined based on the anatomical feature: the stomach, the duodenum (small intestine_1), the jejunum (small intestine_2 ~ small intestine_5), the ileum (small intestine_6), the cecum (large intestine_1), the colon (large intestine_2 ~ large intestine_6), and the rectum (large intestine_7). The anatomical differences between each location are shown in Figure S1.

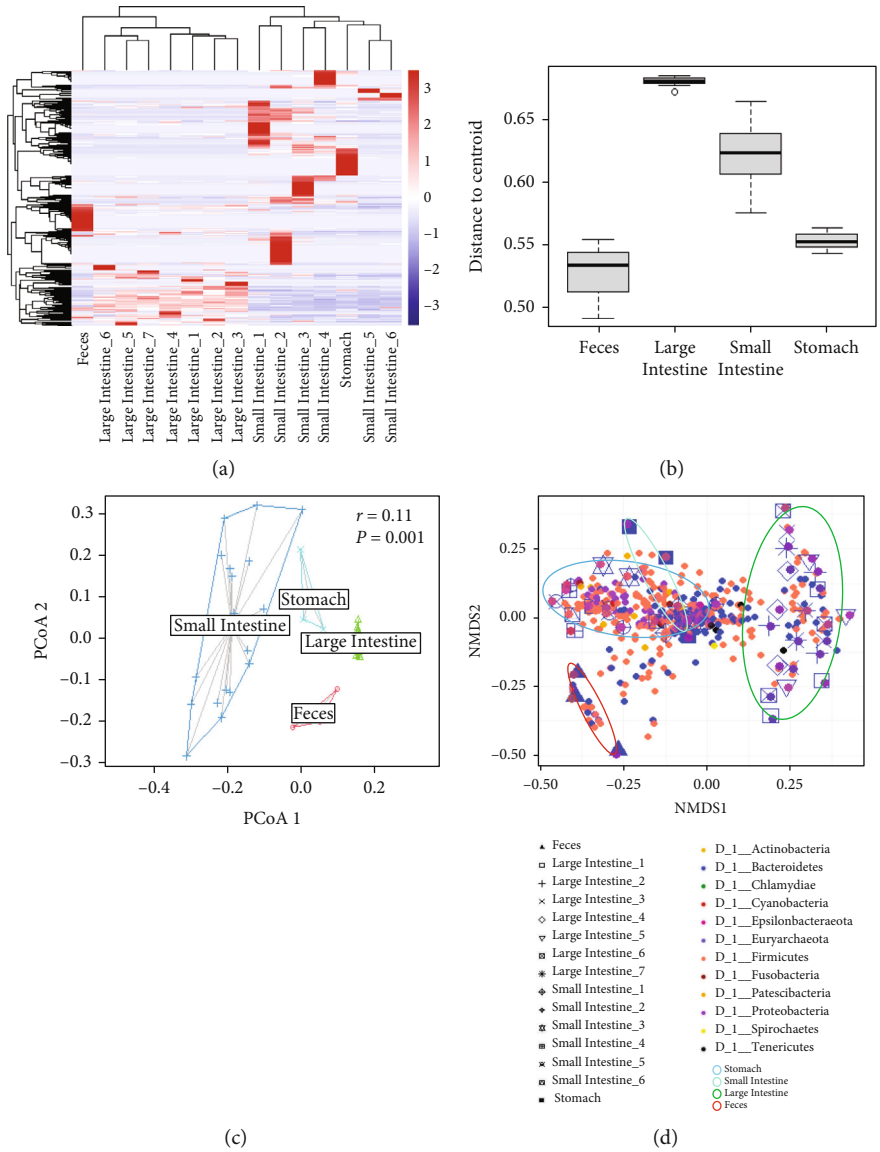

Figure 4: The comparison of microbial diversity at different locations of the GI tracts by β-diversity analysis. (a) Heatmap of the microbial composition and relative abundance in each location of the GI tracts at the genus level based on the Bray-Curtis distance matrix. (b) β-diversity centroid for each GI site. (c) Principal coordinate analysis ($R^2 = 0.11$ and $P = 0.001$). (d) NMDS plots show the difference of microbiome in each location of the GI tracts. The sampling locations within the GI tract were determined based on the anatomical feature: the stomach, the duodenum (small intestine_1), the jejunum (small intestine_2 ~ small intestine_5), the ileum (small intestine_6), the cecum (large intestine_1), the colon (large intestine_2 ~ large intestine_6), and the rectum (large intestine_7). The anatomical differences between each location are shown in Figure S1.

new chemicals while feces, and the stomach contained the least (Figure 5(b)). PCoA showed that the structures of the chemical profiles can be grouped into three categories: the stomach to the small intestine, the large intestine, and feces (Figure 5(c)). An NMDS plot also revealed that the structures of the chemical profiles can be grouped into three categories in accordance with the PCoA analysis result (Figure 5(d) and see Supp. Table 10~11).

3.5. Microbial Cooccurrence Network Analysis Revealed a Convergence of Gut Microbiome in the Large Intestine. We next analyzed the community structure of gut microbiome at each region of the GI tract by cooccurrence network analysis. The network analysis demonstrated remarkable differences in topology and node taxonomic representation depending on the region of the GI tract (Figures 6(a)–6(e)). As expected, the number of bacterial species constituting the gut microbiome at each location was highest in the large intestine (OTUs = 4080) and lowest in the stomach (OTUs = 344) (Figure 6(f)). Despite the small number of bacterial species of the gut microbiome, relatively large numbers of nodes and edges were observed in the stomach (node = 36 and edge = 112), which means that the network of intestinal bacteria in the stomach was not established enough. Interestingly, the nodes and edges of the gut microbiome in the stomach shrunk despite the dramatic increase

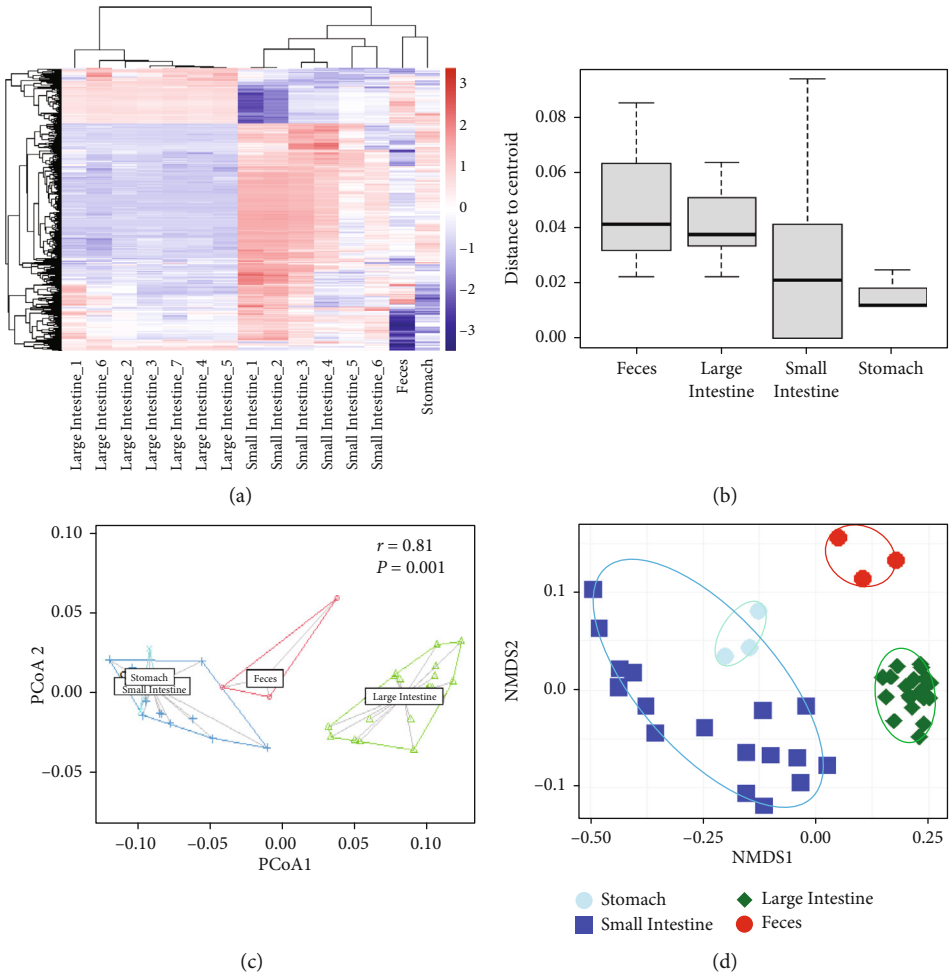

Figure 5: The location-specific chemical diversity in the GI tracts. (a) Heatmap of the chemicals in each location of the GI tracts based on the Bray-Curtis distance matrix. (b) β-Diversity centroid of LC-MS/MS samples from each GI sites. Adonis < 0.001. (c) Similarity of chemical compounds from GI sites based on PCoA, $R^2 = 0.81$, $P = 0.001$. (d) Nonmetric multidimensional scaling (NMDS) plot of the chemicals showing location-specific variation. The relative quantities and identities of chemicals detected by ultra-high-resolution LC-MS/MS in each location of the GI tracts were used for the statistical analyses. The sampling locations within the GI tract were determined based on the anatomical feature: the stomach, the duodenum (small intestine_1), the jejunum (small intestine_2 ~ small intestine_5), the ileum (small intestine_6), the cecum (large intestine_1), the colon (large intestine_2 ~ large intestine_6), and the rectum (large intestine_7). The anatomical differences between each location are shown in Figure S1.

of bacterial species as the gut microbiome transitioned to the large intestine. The gradual decrease of the ratio of nodes and edges to the number of bacterial species from the stomach to the large intestine not only indicates that the network of bacteria was built strongly as the gut microbiome transitioned but also indicates its gradual adaptation. In accordance with the analysis of the gut microbiome profile (Figures 1–4), none of the gut microbiome in the location of the GI tract was like the fecal microbiome.

3.6. Both Water Content and pH Affected the Composition of Gut Microbiome. Since water content and pH are the two main determinants of a physical environment for the proliferation of microbes, we investigated an associative relationship between these factors and the composition of the gut microbiome in each location of the GI tract. As expected, water contents and pH of GI contents were different in a location-specific manner (Figures 7(a) and 7(b)and Supp. Table 12~13). In conformity with the variation of water content and pH in the GI contents, the composition of the gut microbiome varied at each location. Despite the lack of an associative relationship between the main principal component of the gut microbiome and either alone with water content or pH, consideration of both water content and pH with the main principal component showed clear groupings (Figure 7(c)). It should be noted that Figure 7(c) implies that the physical environment of the stomach, i.e. pH and moisture, is very different from the rest of the remaining parts in the GI tract, even from the small intestine along with microbial diversity.

4. Discussion

The gut is a dynamic organ for food digestion; absorption of nutrients, minerals, and water; and excretion of waste metabolites, and its pH and oxygen levels fluctuate

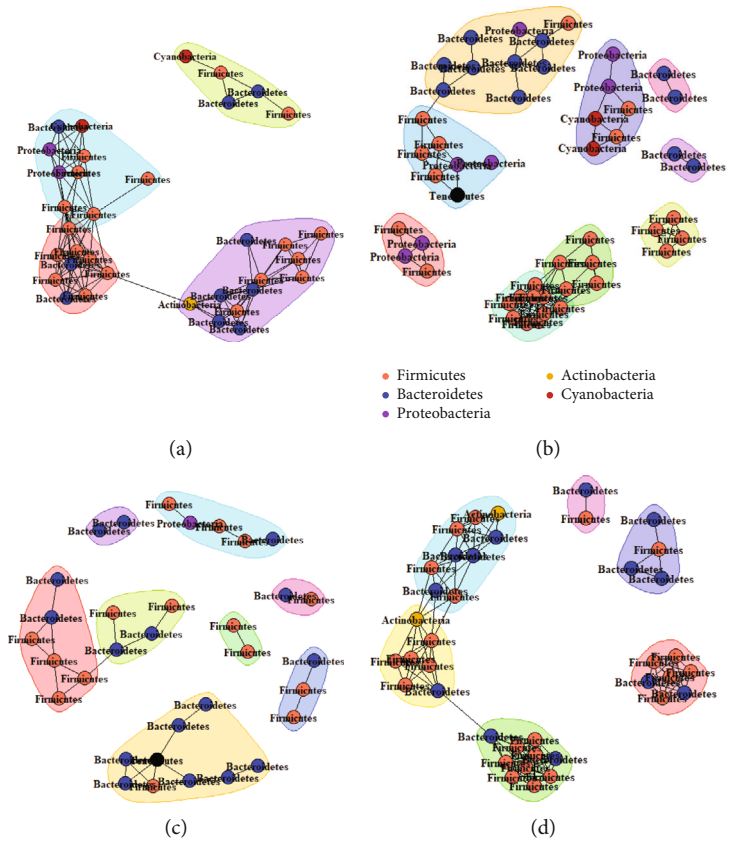

	OTU	Node	Edge	Modularity
Stomach	344	36	112	4
Small Intestine	1337	50	104	9
Large Intestine	4080	33	32	8
Feces	443	39	117	6

(e)

Figure 6: Cooccurrence network analysis of gut microbiome at the stomach (a), the small intestine (b), the large intestine (c) of the GI tract, and feces (d) with the ReBoot algorithm. The colored shapes represent network communities determined by the Louvain modularity algorithm. Node colors and labels represent phyla. (e) The network information of the gut microbiome at the stomach, the small intestine, the large intestine, and feces. OTU: the numbers of OTUs used for network analysis. Node: node numbers. Edge: edge number. Modularity: modularity number. The network was developed by using species-level OTUs.

[25–28]. These activities and functions of the gut are precisely location-specific, which result in location-specific differences of a GI tract [29–33]. In accordance with the previous works, this work showed that the pH, the water content, and the chemical composition differed in a location-specific manner including feces. Considering the location-specific variation of physical and chemical environments in the GI tract, it would be reasonable to assume that the composition of the gut microbiome might fluctuate in a location-specific manner. In fact, this work with genetically homogenous sibling pigs grown in a cohoused condition to minimize experimental errors showed that the composition of the gut microbiome constantly changed in the GI tract, even within the large intestine, in response to the local environmental changes of the GI tract. The location-specific variation of compositional change of gut microbiome including the main dominant bacteria well coincide with variation of chemical and physical factors.

Along with the regional diversity of gut microbiome at the specific location in the GI tract, the number of microbes in the GI content is obviously a main determining factor of the whole gut microbiome in the host. It has been known that the density of intestinal microbes is orders of magnitude higher in the large intestine than in the small intestine [34]. Other than a dense presence of intestinal microbes, the gut microbiome in the large intestine consisted of much diverse kinds of bacterial species. Intestinal bacteria in terms of both species number and their prevalence had been dramatically increased as the intestinal matter transited from the stomach to the large intestine (Figures 1–3). Despite diverse kinds of bacteria in the highest density in the GI tract, the nodes and edges of the microbial cooccurrence network were smaller

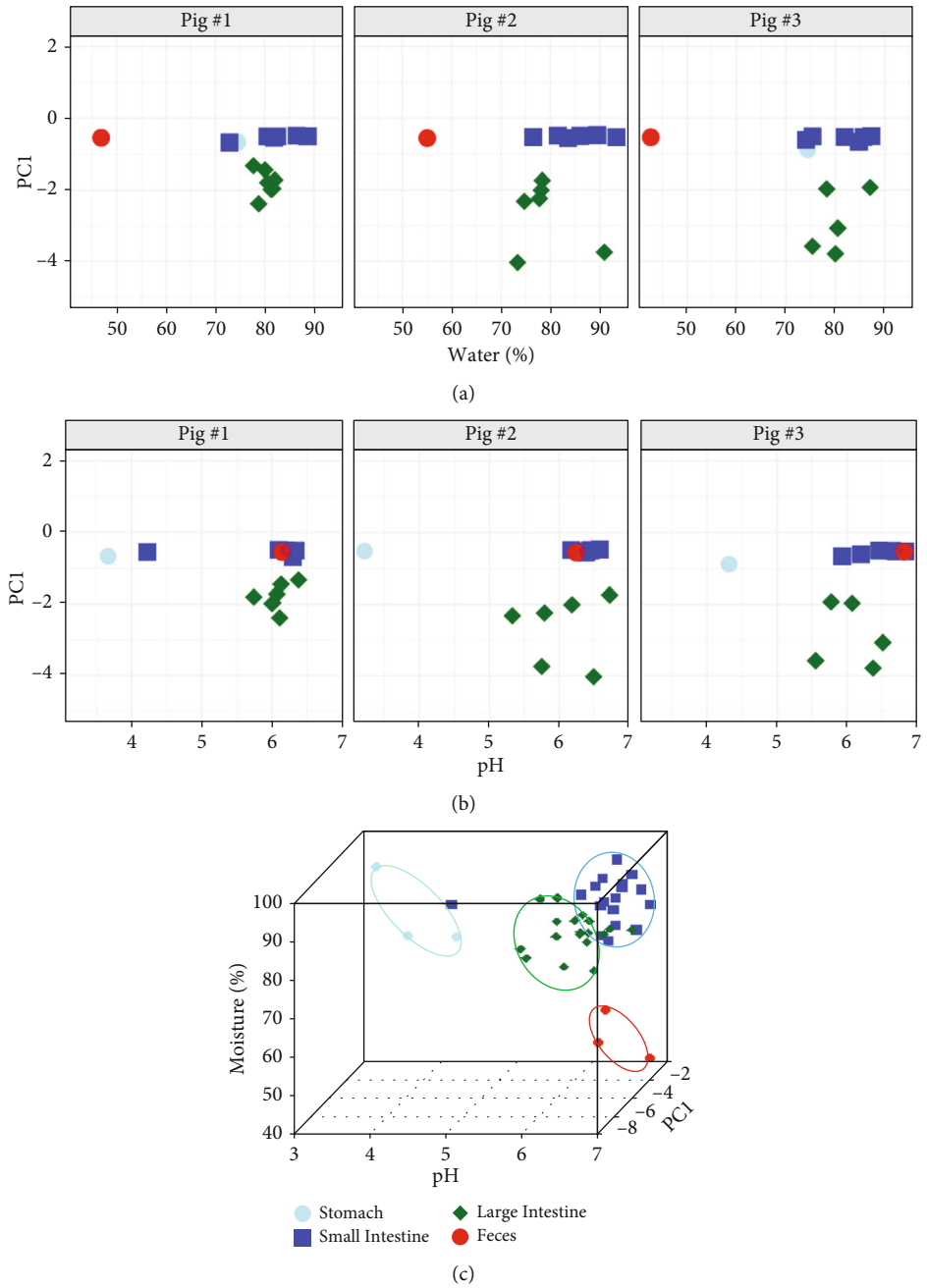

Figure 7: The associative relationship between gut microbiome structure and physical factors. (a) Water content versus the PC1 of gut microbiome. (b) pH versus the PC1 of gut microbiome. (c) 3D plot showing a relationship of water content, pH, and the PC1 of gut microbiome.

than the rest of the other locations of the GI tract (Figure 6). The gradual increase of intestinal microbes which resulted in decrease in the nodes and edges of cooccurrence network showed in this work indicates the gradual adaptation of intestinal microbiome from the stomach to the large intestine. At the same time, the highly dense and diverse bacteria in the large intestine were closely related each other (Figure 6). Besides the close relationship among the intestinal microbes in the large intestine, the topology and node taxonomic representation of the fecal microbiome did not represent any microbiome at the 14 locations. Rather, the topology and node of the fecal microbiome only slightly resembled those of the gut microbiomes within the GI tract including the large intestine, which clearly indicates that fecal microbiome is different from whole gut microbiome.

Recent extensive research on gut microbiome has showed that the intestinal host-microbiome communications play critical roles in determining the phenotypes of its host the development and progression of various diseases especially in liver diseases [3–9]. Despite the determinant role of gut microbiome in the diseases and traits of its host [21, 22, 27, 28, 35], the definite causative intestinal microbes

for the diseases and phenotype have not been identified until now in the contrary to expectation despite extensive research. There could be several reasons for falling short of the expectation: innate feature of metagenome sequencing creating massive sequencing errors, limitation of feces as a proxy to study the whole gut microbiome [22], and errors during stool sampling [15]. There would not be a solution to the limitations of metagenome sequencing and use of fecal gut microbiome as a proxy for the window of the whole gut microbiome at this moment. However, Figure 7 indicates that stool sampling with water content and pH in consideration would reduce errors during analyses in gut microbiome study. Besides the water content, the pH of human feces fluctuates moment to moment within the range of 6.1 ~ 7.9 [30, 36–38]. Since the water content and pH are variable depending on a sampling moment, a consistent collection of stools with the same levels of water content and pH would reduce errors during gut microbiome analyses.

5. Conclusions

This work showed that fecal microbiome has a limited ability to represent all the aspect of the whole gut microbiome of its host. Current gut microbiome research relies on the fecal analysis under the assumption that the fecal microbiome represents the overall profile of the gut microbiome of its host. This work demonstrated that the fecal microbiome does not represent the overall composition of the gut microbiome. Despite the significant roles of gut microbiome in various phenotypes and diseases of its host, the causative microbes for such characteristics identified by one research failed to be reproduced in others. Since fecal microbiome is a mere result of the gut microbiome rather than the representative microbiome of the GI tract of the host as shown here, there is a limitation in identifying causative intestinal microbes related to the phenotypes and diseases by studying fecal microbiome. It seems urgent to develop new methods for gut microbiome analysis, for instance, blood signatures of gut microbiome-based method or endoscopic methods.

Data Availability

The raw data was deposited in the public repository at NCBI SRA with accession number PRJNA707378 (https://submit.ncbi.nlm.nih.gov/subs/sra/).

Conflicts of Interest

The authors declare that they have no competing interests.

Authors' Contributions

S.-T.H., H.-J.K, and H.-J.C. designed the study. J.S.A. and E.L. performed the experiments and analyzed the data. J.S.A. and E.L. performed the statistical analyses. E.L., H.-J.C., H.-J.K, and S.J. assisted with microbiota analyses. All authors contributed to writing or editing to the manuscript. Ji-Seon Ahn and Enkhchimeg Lkhagva contributed equally to this work.

Acknowledgments

This research was funded by the Korea Basic Science Institute (KBSI) grants C210500, C380300, C320000, and C330340 and supported by a grant of the Korea Health Technology R&D Project through the Korea Health Industry Development Institute (KHIDI), funded by the Ministry of Health & Welfare, Republic of Korea (grant number: HV22C0171).

Supplementary Materials

Supplementary 1. Figure S1: the photographs showing the 14 sampling locations in the GI tracts. Supplementary 2. Figure S2: the composition of microbiomes at 4 different locations of the GI tract and feces of pigs #1 ~3.Supplementary 3. Figure S3: heatmap of family level taxonomy in each location of the GI tracts based on the correlation distance matrix. Supplementary 4. Figure S4: the location-specific chemical diversity in the GI tracts. Supplementary 5. Table S1: the row sequencing reads for each sample. Supplementary 6. Table S2: the relative abundance of intestinal bacteria in the fecal matters at the 14 locations of the GI tract and feces in phylum level. Supplementary 7. Table S3: the relative abundance of intestinal bacteria in the fecal matters at the 14 locations of the GI tract and feces in species level. Supplementary 8. Table S4: α-diversity values for microbiome profiles at the 14 locations of the GI tract and feces. Supplementary 9. Table S5: the relative abundance of intestinal bacteria in the fecal matters at the 14 locations of the GI tract and feces in family level. Supplementary 10. Table S6: the average distance to centroid; Table S7: the average distance to NMDS_ microbiota. Supplementary 11. Table S8: the average distance to PcoA_microbiota. Supplementary 12. Table S9: the Shannon α-diversity values for chemical profiles at the 14 locations of GI tract and feces. Supplementary 13. Table S10: the average distance to NMDS_LCMS. Supplementary 14. Table S11: the average distance to PcoA_LCMS. Supplementary 15. Table S12: the water contents at the 14 locations of GI tract and feces. Supplementary 16. Table S13: the pH values at the 14 locations of the GI tract and feces. *(Supplementary Materials)*

References

[1] E. Thursby and N. Juge, "Introduction to the human gut microbiota," *Biochemical Journal*, vol. 474, no. 11, pp. 1823–1836, 2017.

[2] O. Manor, C. L. Dai, S. A. Kornilov et al., "Health and disease markers correlate with gut microbiome composition across thousands of people," *Nature Communications*, vol. 11, no. 1, p. 5206, 2020.

[3] X. Chen, R. D'Souza, and S. T. Hong, "The role of gut microbiota in the gut-brain axis: current challenges and perspectives," *Protein & Cell*, vol. 4, no. 6, pp. 403–414, 2013.

[4] M. Giuffrè, M. Campigotto, G. Campisciano, M. Comar, and L. S. Crocè, "A story of liver and gut microbes: how does the intestinal flora affect liver disease? A review of the literature," *American Journal of Physiology Gastrointestinal and Liver Physiology*, vol. 318, no. 5, pp. G889–G906, 2020.

[5] H. J. Chung, J. G. Yu, I.-A. Lee et al., "Intestinal removal of free fatty acids from hosts by Lactobacilli for the treatment of obesity," *FEBS Open Bio*, vol. 6, no. 1, pp. 64–76, 2016.

[6] Y. Y. Jin, P. Singh, H. J. Chung, and S. T. Hong, "Blood ammonia as a possible etiological agent for Alzheimer's disease," *Nutrients*, vol. 10, no. 5, p. 564, 2018.

[7] J. Liu, E. Lkhagva, H. J. Chung, H. J. Kim, and S. T. Hong, "The pharmabiotic approach to treat hyperammonemia," *Nutrients*, vol. 10, no. 2, p. 140, 2018.

[8] T. T. B. Nguyen, Y. Y. Jin, H. J. Chung, and S. T. Hong, "Pharmabiotics as an emerging medication for metabolic syndrome and its related diseases," *Molecules*, vol. 22, no. 10, p. 1795, 2017.

[9] T. T. B. Nguyen, H. J. Chung, H. J. Kim, and S. T. Hong, "Establishment of an ideal gut microbiota to boost healthy growth of neonates," *Critical Reviews in Microbiology*, vol. 45, no. 1, pp. 118–129, 2019.

[10] C. Duvallet, S. M. Gibbons, T. Gurry, R. A. Irizarry, and E. J. Alm, "Meta-analysis of gut microbiome studies identifies disease-specific and shared responses," *Nature Communications*, vol. 8, no. 1, p. 1784, 2017.

[11] E. Rinninella, P. Raoul, M. Cintoni et al., "What is the healthy gut microbiota composition? A changing ecosystem across age, environment, diet, and diseases," *Microorganisms*, vol. 7, no. 1, p. 14, 2019.

[12] W. A. Walters, Z. Xu, and R. Knight, "Meta-analyses of human gut microbes associated with obesity and IBD," *FEBS Letters*, vol. 588, no. 22, pp. 4223–4233, 2014.

[13] E. F. Tigchelaar, M. J. Bonder, S. A. Jankipersadsing, J. Fu, C. Wijmenga, and A. Zhernakova, "Gut microbiota composition associated with stool consistency," *Gut*, vol. 65, no. 3, pp. 540–542, 2016.

[14] D. Vandeputte, G. Falony, S. Vieira-Silva, R. Y. Tito, M. Joossens, and J. Raes, "Stool consistency is strongly associated with gut microbiota richness and composition, enterotypes and bacterial growth rates," *Gut*, vol. 65, no. 1, pp. 57–62, 2016.

[15] L. Vork, J. Penders, J. Jalanka et al., "Does day-to-day variability in stool consistency link to the fecal microbiota composition?," *Frontiers in Cellular and Infection Microbiology Cell*, vol. 11, article 639667, 2021.

[16] W. A. James, E. Ogunrinde, Z. Wan et al., "A distinct plasma microbiome but not gut microbiome in patients with systemic lupus erythematosus compared to healthy individuals," *The Journal of Rheumatology*, vol. 49, no. 6, pp. 592–597, 2022.

[17] E. Lucchinetti, P.-H. Lou, P. Lemal et al., "Gut microbiome and circulating bacterial DNA ("blood microbiome") in a mouse model of total parenteral nutrition: Evidence of two distinct separate microbiotic compartments," *Clinical Nutrition ESPEN*, vol. 49, pp. 278–288, 2022.

[18] J. P. Rowan, K. L. Durrance, G. E. Combs, and L. Z. Fisher, "The digestive tract of the pig," *Animal Science Department, Florida Cooperative Extension Service, Institute of Food and Agricultural Sciences, University of Florida, Gainesville, Document AS23*, vol. 1, pp. 1–3, 2015.

[19] S. N. Heinritz, R. Mosenthin, and E. Weiss, "Use of pigs as a potential model for research into dietary modulation of the human gut microbiota," *Nutrition Research Reviews*, vol. 26, no. 2, pp. 191–209, 2013.

[20] D. S. Kim, K.-E. Park, Y.-J. Kwak et al., "Agrimonia pilosaLedeb root extract: anti-inflammatory activities of the medicinal herb in LPS-induced inflammation," *The American Journal of Chinese Medicine*, vol. 48, no. 8, pp. 1875–1893, 2020.

[21] E. Lkhagva, H. J. Chung, J. S. Ahn, and S. T. Hong, "Host factors affect the gut microbiome more significantly than diet shift," *Microorganisms*, vol. 9, no. 12, p. 2520, 2021.

[22] E. Lkhagva, H. J. Chung, J. Hong et al., "The regional diversity of gut microbiome along the GI tract of male C57BL/6 mice," *BMC Microbiology*, vol. 21, no. 1, 2021.

[23] J. Oksanen, F. G. Blanchet, M. Friendly et al., "Vegan: community ecology package. R package version 2.5-7," 2020, https://github.com/vegandevs/vegan.

[24] P. J. McMurdie and S. Holmes, "phyloseq: an R package for reproducible interactive analysis and graphics of microbiome census data," *PLoS One*, vol. 8, no. 4, article e61217, 2013.

[25] A. Brune, "Termite guts: the world's smallest bioreactors," *Trends in Biotechnology*, vol. 16, no. 1, pp. 16–21, 1998.

[26] A. Brune and M. Friedrich, "Microecology of the termite gut: structure and function on a microscale," *Current Opinion in Microbiology*, vol. 3, no. 3, pp. 263–269, 2000.

[27] H. J. Chung, T. T. B. Nguyen, H. J. Kim, and S. T. Hong, "Gut microbiota as a missing link between nutrients and traits of human," *Frontiers in Microbiology*, vol. 9, p. 1510, 2018.

[28] D. R. Pandeya, R. D'Souza, M. M. Rahman, S. Akhter, H. J. Kim, and S. T. Hong, "Host-microbial interaction in the mammalian intestine and their metabolic role inside," *Biomedical Research*, vol. 23, no. 1, pp. 9–21, 2012.

[29] R. Bown, G. Sladen, M. Clark, and A. Dawson, "The production and transport of ammonia in the human colon," *Gut*, vol. 12, no. 10, p. 863, 1971.

[30] J. B. Dressman, R. R. Berardi, L. C. Dermentzoglou et al., "Upper gastrointestinal (GI) pH in young, healthy men and women," *Pharmacuetical Research*, vol. 7, no. 7, pp. 756–761, 1990.

[31] L. Kalantzi, K. Goumas, V. Kalioras, B. Abrahamsson, J. B. Dressman, and C. Reppas, "Characterization of the human upper gastrointestinal contents under conditions simulating bioavailability/bioequivalence studies," *Pharmaceutical Research*, vol. 23, no. 1, pp. 165–176, 2006.

[32] L. C. McGee and A. B. Hastings, "The carbon dioxide tension and acid-base balance of jejunal secretions in man," *Journal of Biological Chemistry*, vol. 142, no. 2, pp. 893–904, 1942.

[33] S. J. Rune, "Acid-base parameters of duodenal contents in man," *Gastroenterology*, vol. 62, no. 4, pp. 533–539, 1972.

[34] G. P. Donaldson, S. M. Lee, and S. K. Mazmanian, "Gut biogeography of the bacterial microbiota," *Nature Reviews Microbiology*, vol. 14, no. 1, pp. 20–32, 2016.

[35] K. J. Portune, A. Benitez-Paez, E. M. Del Pulgar, V. Cerrudo, and Y. Sanz, "Gut microbiota, diet, and obesity-related disorders–the good, the bad, and the future challenges," *Molecular Nutrition Food Research*, vol. 61, no. 1, article 1600252, 2017.

[36] D. Evans, G. Pye, R. Bramley, A. G. Clark, T. J. Dyson, and J. D. Hardcastle, "Measurement of gastrointestinal pH profiles in normal ambulant human subjects," *Gut*, vol. 29, no. 8, pp. 1035–1041, 1988.

[37] J. Fallingborg, L. A. Christensen, M. Ingeman-Nielsen, B. A. Jacobsen, K. Abildgaard, and H. H. Rasmussen, "pH-profile and regional transit times of the normal gut measured by a radiotelemetry device," *Alimentary Pharmacology and Therapeutics*, vol. 3, no. 6, pp. 605–614, 1989.

[38] H.-J. Chung, E. Lkhagva, S. Jung, H.-J. Kim, and S.-T. Hong, "Fecal microbiome does not represent whole gut microbiome," *Research Square*, 2022.